Technical University of Denmark

Analysis of long distance wakes of Horns Rev I using actuator disc approach

Eriksson, O.; Mikkelsen, Robert Flemming; Hansen, Kurt Schaldemose; Nilsson, Karl ; Ivanell, S.

Published in:
Journal of Physics: Conference Series (Online)

Link to article, DOI:
10.1088/1742-6596/555/1/012032

Publication date:
2014

Document Version
Publisher's PDF, also known as Version of record

Analysis of long distance wakes of Horns Rev I using actuator disc approach

2014 J. Phys.: Conf. Ser. 555 012032

(http://iopscience.iop.org/1742-6596/555/1/012032)

Analysis of long distance wakes of Horns Rev I using actuator disc approach

O Eriksson[1,2], R Mikkelsen[3], K S Hansen[3], K Nilsson[1,2], S Ivanell[1,2]
[1]Wind Energy Campus Gotland, Dep. of Earth Sciences, Uppsala University, 621 67, Visby, Sweden
[2]KTH, Stockholm, Sweden
[3]DTU, Lyngby, Denmark

E-mail: ola.eriksson@geo.uu.se

Abstract. The wake recovery behind the Horns Rev wind farm is analysed to investigate the applicability of Large Eddy Simulations (LES) in combination with an actuator disc method (ACD) for farm to farm interaction studies. Periodic boundary conditions on the lateral boundaries are used to model the wind farm (as infinitely wide), using only two columns of turbines. The meteorological conditions of the site are taken into account by introducing wind shear and pre-generated synthetic turbulence to the simulation domain using body forces. Simulations are carried out to study the power production and the velocity deficit in the farm wake. The results are compared to the actual power production as well as to wind measurements at 2 km and 6 km behind the wind farm. The simulated power production inside the farm shows an overall good correlation with the real production, but is slightly overpredicted in the most downstream rows. The simulations overpredict the wake recovery, namely the wind velocity, at long distances behind the farm. Further studies are needed before the presented method can be applied for the simulation of long distance wakes. Suggested parameters to be studied are the development of the turbulence downstream in the domain and the impact of the grid resolution.

1. Introduction

Behind every large offshore wind farm a long distance wake will be found. As more offshore wind farms are built there will be more occasions when the wake from one wind farm will interact with other nearby wind farms. This makes it interesting to study not only the near and far wakes behind single turbines and the interaction inside wind farms but also the long distance wakes impacting the wind conditions at neighboring sites.

As a first step towards better understanding of farm to farm interaction the wake recovery needs to be predicted accurately. Knowledge can be gained from both numerical simulations of and measurements in the wake, however, modeling of very long wakes using computational fluid dynamics (CFD) is subject to increased uncertainty.

The present work studies the farm wake using Large Eddy Simulations (LES) of Horns Rev I (hereafter denoted as Horns Rev), an offshore wind farm west of Denmark with 80 turbines. Horns Rev, whose layout is presented in figure 1, consists of 80 wind turbines in 10 rows (7 degrees (deg) turned from North-South) and 8 columns (West-East). The internal spacing between the turbines in the rows and columns is 7 rotor diameters (D), making the farm about 4 km wide and 5 km long.

Two met towers situated 2 km and 6 km east of the wind farm make the farm ideal for studies of the wake velocity deficit over longer distances. Horns Rev has long term measurements from both met masts which show a clear recovery in the long distance wake. The measurements are taken by met masts at hub height and filtered to correspond to the simulated cases. For the same cases filtered production data for the wind turbines are also available.

The simulations are done using an actuator disc (ACD) method. By using periodic boundary conditions on the lateral boundaries the simulations can be done using only 20 turbines. This decreases the needed computational power as the boundary layers of the blades are not resolved and the farm is not simulated in its whole width. This allows more resources to be used for simulation of the wake. However, due to the large simulated distance behind the farm the needed computational power is still quite large.

Earlier studies of wake recovery behind Horns Rev have also been done using simplified wake models which are compared to measurements, see Frandsen [1], see Brand [2]. These studies include models using the momentum equation, roughness elements representing the turbines or CFD. LES were discussed but disregarded at the time due to the needed computational power.

CFD studies employing the actuator disc methodology with LES have later been carried out on the Horns Rev wind farm by Ivanell [3]. The used methods are the same as in this study, but with some differences in input and grid, see chapter 3.3. The simulations by Ivanell were done to study the reduced energy production due to wakes inside the farm. The simulations showed fairly good correlation concerning the power production inside the farm.

This study will complement the earlier work done by Ivanell by studying the very far wake behind the wind farm. By comparing the velocity deficit from the simulation result with the measured velocity deficit, the performance of the model on large distances behind the farm is evaluated.

The performance inside the farm is also studied to validate the method. The production results from the simulated cases are compared to the measured production. A comparison is also done to see how well this simulation models the farm compared to the earlier study using the same method.

To be able to study the wake recovery behind the wind farm a much larger domain downstream is needed compared to earlier studies. The grid needs to include both the wind farm and the met mast.

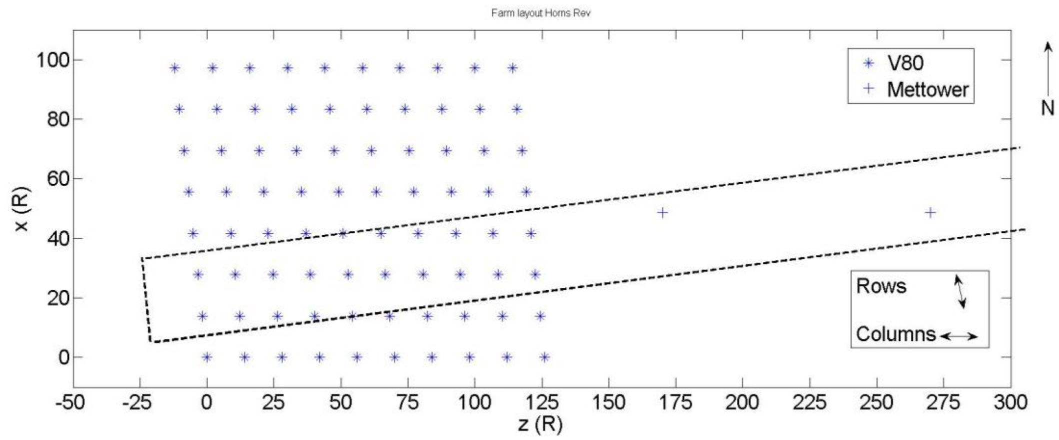

Figure 1. Horns Rev consists of 80 Vestas V80 wind turbines in 10 rows and 8 columns. Two met masts are situated east of the farm. An approximation of the grid used for the simulation is marked.

2. Measurement data

Long term wind data from Horns Rev are available from measurements conducted at 2 km and 6 km east of the wind farm. The measurement methodology and the available data sets are presented in an UPWIND report, by Hansen [4]. The data sets consist of 10 minute mean values from measurements performed before the second wind farm Horns Rev II was erected. The measurements are filtered to give data that correspond to the simulated cases i.e., all turbines are available and there is a stationary flow during the 10 minute averaged period. For this study the data are filtered for a flow direction of 270±2.5 degrees and a wind speed of 6, 8 and 10 m/s in an interval of ±0.5 m/s.

Measurements were also taken at the site before the erection of the Horns Rev I giving information about the background turbulence level and the wind shear at the site.

3. Simulation method and input

LES are performed in order to estimate the production in the farm and the velocity deficit in the very far wake. The simulations are performed in accordance to the turbulence and wind shear conditions of the site. A neutral atmosphere is assumed. The result is also compared to measured production data and wind data in the wake.

3.1. Numerical model

A LES of Navier-Stokes equations (NS) (1) in general curvilinear coordinates is conducted using a finite volume discretization. The simulations are performed with Ellipsys3D, a general purpose flow solver developed at DTU and Risø, see Sørensen [5] and Michelsen [6], [7]. The grid has a multi block structure allowing the simulations to be parallelized with Message Passing Interface (MPI) and solved with multiple processors at a cluster. The code is formulated in the primitive variables pressure and velocity which are collocated in the cell center. Therefore Rhie/Chow interpolation is used to avoid odd/even pressure decoupling. Using the coordinate directions (x_1, x_2, x_3) the Navier-Stokes equations are formulated as:

$$\frac{\partial u_i}{\partial t} + \frac{\partial u_i u_j}{\partial x_j} = \frac{1}{\rho}\frac{\partial p}{\partial x_i} + f_{body,i} + \frac{\partial}{\partial x_j}\left[(\nu + \nu_t) * \left(\frac{\partial u_i}{\partial x_j} + \frac{\partial u_j}{\partial x_i}\right)\right], \quad \frac{\partial u_i}{\partial x_i} = 0 \qquad (1)$$

where u_i is the velocity vector, p is the pressure, t is time and ρ is the density of air and f_{body} represent the forces added in the domain, ν is the kinematic viscosity, and ν_t is the eddy viscosity that is modeled through the sub-grid-scale model, by Ta Phouc [8].

The numerical method used in the solver is a third order QUICK (Quadratic Upstream Interpolation for Convective Kinematics) for the convective terms (10%) and a fourth order CDS (Central Difference Scheme) for the diffusive terms (90%).

The actuator disc is implemented by adding body forces on a disc representing the rotor, see Mikkelsen [9]. The forces are added on a finer polar grid that is interpolated to the main Cartesian grid. To avoid singularities in the calculations Gaussian smearing distributes the forces to the neighboring nodes in the stream wise direction and in 3D at the tip of the blade.

Turbulence is implemented as fluctuating volume forces that are added in a 2D plane before the first rotor and convected down stream in the domain. The forces are generated from the Mann model, see Mann [10], that calculates fluctuations in the velocities for a certain turbulence level. Also these forces are distributed using Gaussian smearing.

A desired wind shear is applied in the entire domain by a simulation step in which body forces are imposed, see Mikkelsen [11]. These body forces are used in the LES together with the forces representing the turbulence and the wind turbines.

3.2. Numerical setup

The numerical grid consists of a number of blocks and each block consists of a number of cells in each direction. The used grid depends on the distribution of the wind farm, turbine size, the needed resolution for the rotor disc and computational requirements. The simulations also need to be adjusted according to the experimental data from the site considering both turbulence and wind shear. Finally the body forces representing the rotor need to be in accordance with the used turbine and the simulated case.

3.2.1. Grid and boundary conditions. To decrease the needed computational resources a grid is chosen that can be repeated using periodic boundary condition at the lateral boundaries to represent an infinitely wide wind farm. Here the wind farm is rotated 7 degrees, causing the incoming wind from the left to be from 263 degree, see Figure 2.

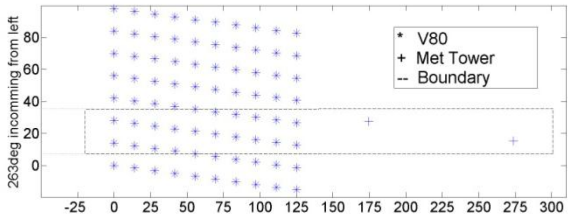

Figure 2. The layout of the Horns Rev wind farm turned 7 degrees clockwise. The rectangle shows the part covered by the grid [R].

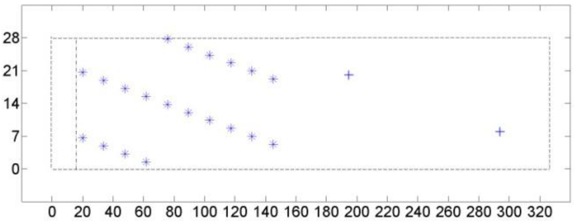

Figure 3. The grid used at the used coordinates [R]. The line at z = 16 shows the turbulence plane.

The grid is centered around the center line between the met towers in the x-direction (span wise) and covers two columns, 28 rotor radii (R). The simulation can be performed for inflow angles between approximately 257 degrees and 280 degrees without any impact due to the use of an infinitely wide farm created by the periodic boundary condition. The most critical impact is on the most distant met tower in the simulation and originates from the “imaginary” turbine at the coordinate (0, -7).

In the stream wise direction (z) the grid starts 20 R before the first turbine and extends 326 R, covering the met mast at 294 R with some margin. In Figure 3 the simulated turbines and the positions in the used grid are shown.

The boundary condition used in the inlet is constant value (Dirichlet) with the resulting wind speed (normalized to 1) divided into wind vectors in the x and z directions. The top boundary condition is set to far field and the bottom boundary condition is set to no slip/wall. For the outlet a convective boundary condition is used.

The resolution of the grid is chosen to be around 20 grid points over the rotor. The exact grid resolution is based on an equidistant grid in the x-direction. The cell size of 0.1094 R is given from the grid’s 4 blocks of 64^3 cells in the span wise direction covering 28 R, see Figure 5. In the y-direction one block is used, the cell size is equidistant in the lower levels and stretched to the upper boundary. In the z-direction the stretching is done up to 15 R and after that the cells are equidistant, see Figure 6.

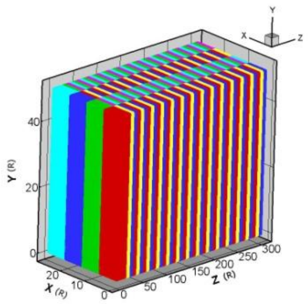

Figure 4. The grid consisting of 4 blocks in the span wise, 1 block in the vertical and 42 blocks in the stream wise direction.

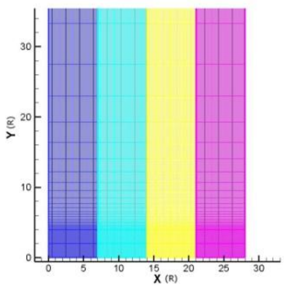

Figure 5. The grid with equidistant cell spacing in the span wise and in the vertical direction up to 4.5 R. The vertical direction is thereafter stretched up to 50 R.

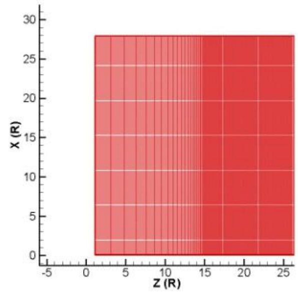

Figure 6. The grid with equidistant cell spacing in the span wise direction. In the stream wise direction the grid is stretched up to 15 R and is thereafter equidistant.

The total number of blocks in the z direction is dependent on the structure of the cluster that uses 8 processors per node. Using 42 blocks the grid covers the met towers and can be run in parallel on 21 nodes in the cluster.

The total number of blocks is 168 (1∗4∗42) and each block consists of 64^3 cells giving a grid of totally 44 million mesh points, see Figure 4.

3.2.2. Wind shear and turbulence. Body forces are introduced in the domain to reach a desired wind shear. The conditions of the site are taken from the measurements done before the erection of the turbines and the known condition of the ground. Here the same values are used as in the simulations of Ivanell. At different heights the wind (w) is described with different wind shears. The input values used in the expression below are Δ = 0.4 R and the shear exponent α = 0.15. The parameter w_0 describes the wind at hub height and c_1, c_2 describe the wind shear for lower heights.

$$w(y) = \begin{cases} w_0.(c_2 y^2 + c_1 y) & y \leq \Delta \\ w_0.\left(\frac{y}{h_{hub}}\right)^{\alpha} & y > \Delta \end{cases} \qquad (2)$$

Turbulence is implemented as fluctuating body forces that are added in a 2D plane at 16 R in the z-direction, inside the equidistant region but still in front of the first rotor, see Figure 3. The forces are generated by the Mann model that uses rapid distortion theory to generate a homogenous turbulence field. The turbulence level that is generated gives a resulting horizontal turbulence level of 4.7%. The turbulence box has a width of 28 R, height of 5 R and depth of 900 R. The same turbulence field has been used for all of the three simulated directions.

Compared to the site condition measured before the erection of Horns Rev the turbulence intensity for the given directions were around 7% for all directions and wind speeds, see Hansen [12].

3.2.3. Turbine and Airfoil data. The turbines used at Horns Rev are Vestas V80s, with an 80 m rotor diameter and a hub height of 70 m. The shaft tilt-up angle is 6 degrees. The turbine has a rated power of 2 MW.

The turbine is modeled by an ACD method using lift and drag coefficients (C_L, C_D) tabulated as a function of the angle of attack and Reynolds number, for each type of profile of the blade. A generic turbine design is used as all airfoil data for the real turbine of Horns Rev are not available. The generic Vestas V80 design giving the C_L and C_D is based on the generic Siemens SWT-2.3-93 design with information for the control system (the control system is not used in the simulation) and blade design, see Matthew [13]. The power curve for the turbines of Horns Rev is known. Between 5.4 m/s and 9.5 m/s the tip speed ratio is 8.4. At least the measurement data for 6 and 8 m/s could then be compared to the same simulation. For 10 m/s the tip speed ratio is around 8.

The forces of the rotor are distributed on a polar grid with 21 point in the radial direction and 81 points in the azimuthal direction. The forces are interpolated to the Cartesian grid. To avoid singularities the body forces are smeared to the neighboring nodes.

3.2.4. Simulation time and averaging. The needed simulation time is dependent first on the time it takes for the turbulence to be distributed through the entire domain and secondly on the needed time to average over to get a quasi stable solution.

The time step of the solution needs to be fine enough to fulfill the CFL-condition (3) defined as:

$$\frac{U_0 * \Delta t}{\Delta x} < 1 \qquad (3)$$

Where U_0, equal to 1, is the incoming velocity normalized, as all velocities in the simulation, by the free stream velocity and the grid resolution Δx is 0.1094. This gives an allowed value of $\Delta t < 0.1094$. In the simulation a conservative time step (Δt) of 0.025 is used.

The length to the most distant met mast from the turbulence plane is 273 R. Counting with the lowest incoming wind speed (U) 6 m/s the desired time for the turbulence to be distributed is 1820 seconds. The computational time has a relation to the physical time as in (4) which gives the desired computational time 273 seconds or 11000 time steps.

$$\Delta t_{physical} = \Delta t_{computational} * \frac{R}{U} \tag{4}$$

The whole turbulence box used will pass in about 36000 time steps. The needed computational resources are too high to use the whole box. For the wind speed (U) 6/8/10 m/s a 10 minute average corresponds to averaging over 3600/4800/6000 time steps. In Figure 7 the C_p values for 270 degrees are shown for averaging over 1000-9000 time steps with the start point at 11000 steps. When averaging over a few thousand time steps the variations depending of the number of steps averaged over are large. The difference between the averaging over 9000 or 10000 steps is small, which is why an averaging over 9000 time steps is used in the results. For the 6/8/10 m/s this corresponds to 2.5/1.9/1.5 periods of 10 minutes.

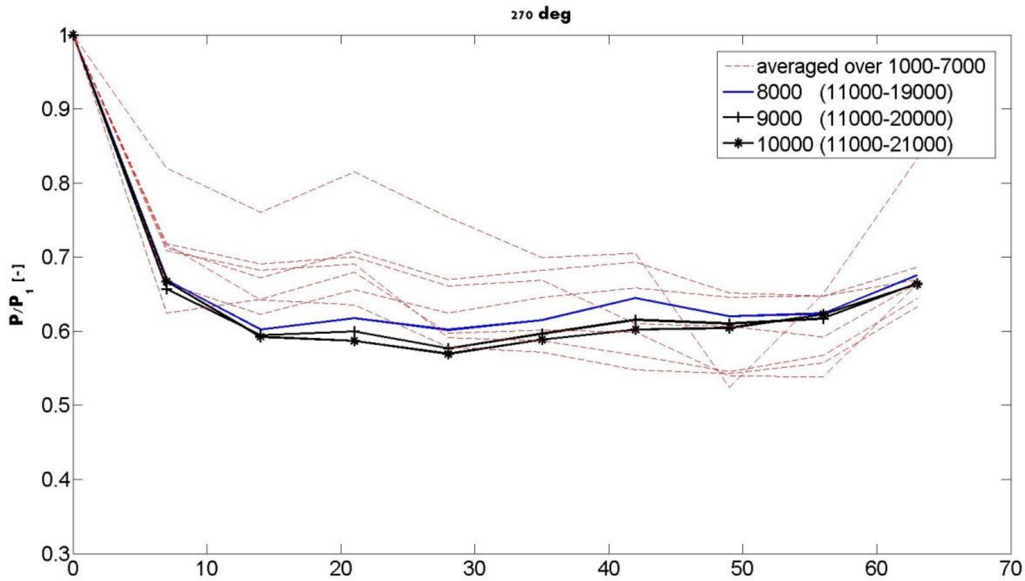

Figure 7. C_P value for the simulation of 270 degrees for different averaging times (from 1000-10000 time steps) starting from 11000 time steps.

3.2.5. Direction Averaging and height interpolation. The simulations will be compared to the measurement data for the sector 270±2.5 degrees. The simulation result that is compared to the measured data is based on the three simulations done for 267.5, 270 and 275 degrees. The simulation result is averaged as the mean value of the three simulations.

For the data logged at the position of the met towers no cell corresponds to the actual hub height, 1.76 R. A linear interpolation is done between the closest cells in the y-direction to get a value comparable to the height of the measured data.

3.3. Numerical setup compared to earlier study
Earlier simulations of Horns Rev with the same model, as described earlier, were done by Ivanell [3]. A comparison of the simulation setup between this and the earlier simulation shows some differences but is also similar in many aspects.

The grid has the same extension in x- and y-direction and the rotation of the grid is the same. The used wind shear is the same as is the boundary conditions for the grid.

Some of the differences are which turbines are inside the grid (the grids placement in the x-direction in relation to the wind turbine placement) and the length of the domain in the z-direction as this study is extended to simulate the long distance wake as well and therefore needs to include the met towers in the domain. The turbulence data differs in value, 3.1 % compared to 4.7% in this study, as well as of how long the turbulence box is. Finally different airfoil data are used for the V80 for the actuator disc method.

4. Results
The main interest of this study is the simulation result of the wake recovery at long distances behind the wind farm, e.g. the wind speeds at the met towers' positions to be able to validate the model prediction and the uncertainty of the results compared to the measured values. To validate the model a comparison is also done between the measured and the simulated production of the wind turbines.

The first output from the simulation result that is used consists of the power coefficient for the inserted turbines. For each point the velocities in x, y and z direction are also available. The wind speeds are tracked for each step in the calculation for the points corresponding to the place of the met towers.

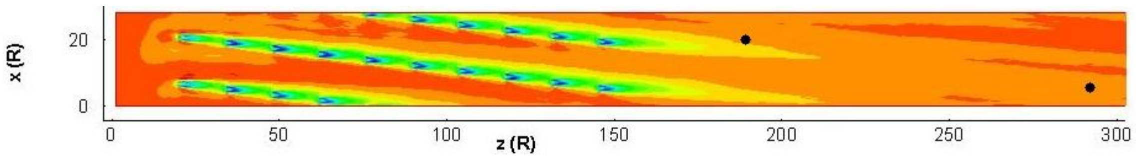

a)Velocity plots mean 267.5 degrees

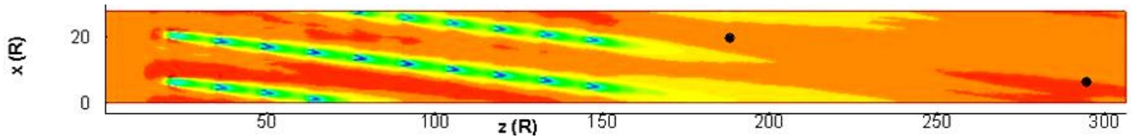

b)Velocity plots mean 270 degrees

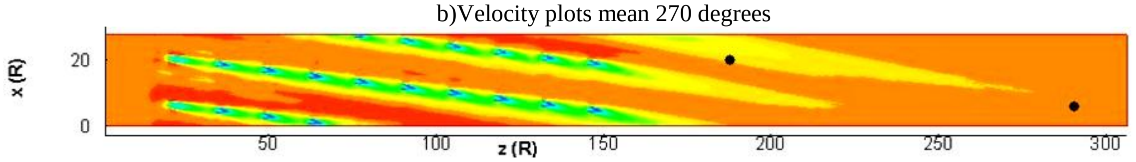

c)Velocity plots mean 272.5 degrees

Figure 8. Averaged wind speeds for the three different simulation cases, from the top (a) 267.5 degrees, (b) 270 degrees and (c) 272.5 degrees. The black dots illustrate the met towers.

4.1. Simulations.
This study has a focus on the wind direction sector of 270±2.5 deg. The simulations are done for the inflow wind speed to the farm of 6, 8 and 10 m/s. In Figure 8 the directions of the mean velocity of the wakes can be seen for the different inflow angles.

The tip speed ratio is about the same for the three wind speeds, that means that the simulation result will be the same for all three wind speeds (for 10 m/s it may be slightly lower) as the incoming wind always is normalized to 1 in the simulations. Three simulations are performed for the angles 267.5, 270 and 272.5 degrees.

4.2. Comparison to measured production

The production of the wind turbines in Figure 9 shows the production along the column of turbines normalized with the production of the first turbine. For the measured data, the values correspond to the mean values for each row, see Figure 1. The simulated data for the values are however taken for the column that is fully covered by the domain.

The simulations capture the production very well for the first rows but tend to overestimate the production for further downstream rows. The inflow angle of 270 degrees with full wake situations gives values closer to the measured result.

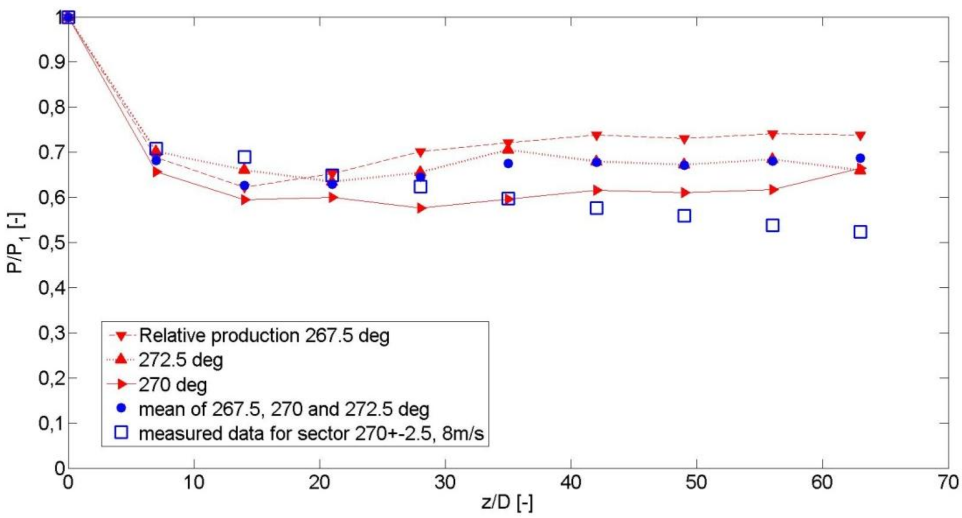

Figure 9. Simulated production values and comparison to the measured data.

4.3. Comparison to prior simulations of production

Earlier simulations of Horns Rev with the same model were done by Ivanell [3]. The result for the earlier simulation for the sector 270 degrees shows a lower production compared to this simulation.

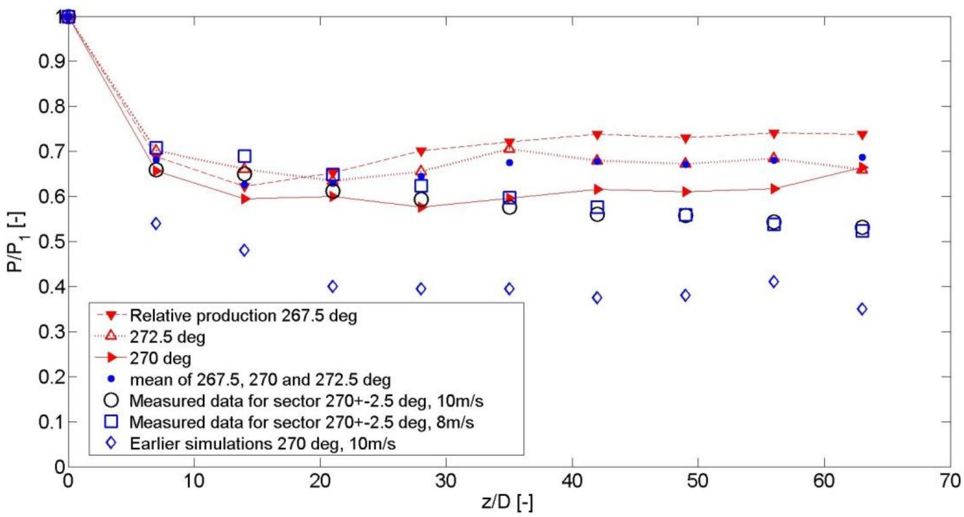

Figure 10. Simulated production values and comparison to earlier simulations.

4.4. Comparison to measured wake recovery

The simulation data are logged for the two mast positions and averaged from step 11000 until step 20000. The simulated velocities for the stream wise direction are presented in Figure 11 and show at the closest met mast a recovery of around 95% of the incoming wind and for the more distant mast a full recovery. A comparison with the measured data, for the same place and height, shows a lower recovery rate. At the closest mast the measured velocity has recovered to 84-89% depending on the incoming wind and for more distant mast to 88-96%.

Remembering the comparison of the production inside the farm some overestimation of the wake recovery was expected.

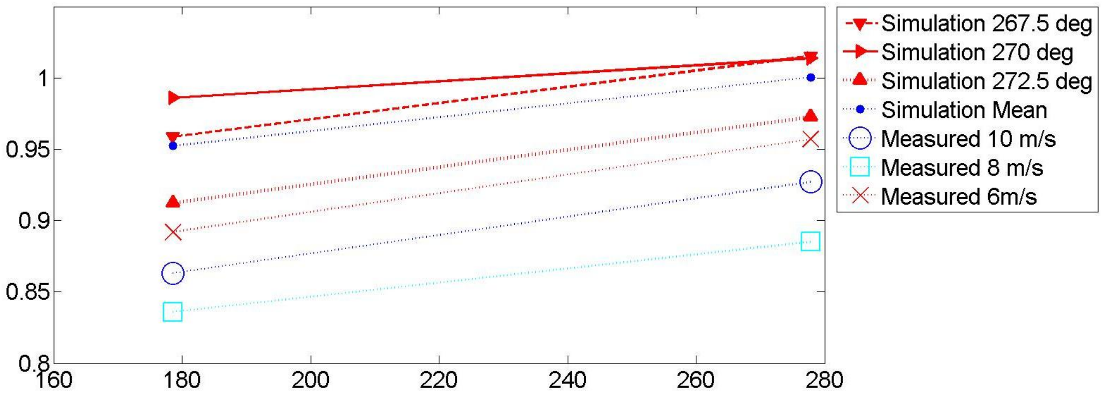

Figure 11. Comparison between the simulated and the measured wind speeds at the two met masts in relation to the incoming wind.

5. Conclusion

LES are done in EllipSys3D using the actuator disc approach to study the ability of the model to simulate the wake recovery in the long distance wake behind large offshore wind farms. To reduce the computational power only a part of the width has been simulated with periodic boundary conditions. For the simulated inflow angle this solution will be valid.

The simulation results show good correlation for the prediction of the power production inside the wind farm although some overprediction is seen for the downstream rows. Looking at the wake recovery at long distance the recovery rate is higher in the simulations compared to the measured data.

The parameters in the simulation that have an impact on the result are related to the numerical model or the physical description. Parameters that are related to the numerical model are for example the grid resolution, time step and Reynolds number. The physical parameters are limited to the wind shear and the turbulence level.

The deviation between the measured and simulated result can have different causes and needs further investigation. The higher recovery for the downstream rows of the farm and in the farm wake seems to indicate that the mixing is higher in the simulations compared to the measurement. In comparison to simulations inside the wind farm we here have a longer domain and therefore also a longer simulation time. Further studies need to be done to see if the used grid resolution and Reynolds number are sufficient to avoid too much numerical diffusion and to investigate to what extent the introduced turbulence intensity is preserved in a physical manner throughout the whole domain.The implementation of the wind shear and the turbulence are other factors to consider. A reason for the deviation can also be how well the filtered measurement data correspond to the simulated cases or should, for example, a larger variation of inflow angle be assumed.

Acknowledgments
The simulations were performed on resources provided by the Swedish National Infrastructure for Computing (SNIC) at the National Supercomputer Centre in Sweden (NSC)

References

[1] Frandsen S, Barthelmie R, Rathmann O, Jørgensen H E, Badger J, Hansen K, Ott S, Rethore P E, Larsen S E, Jensen L E, *Summary report: The shadow effect of large wind farms:measurements,data analysis and modelling',* Risø-R-1615(EN), Denmark 2007.
[2] Brand A J, *Wind Power Plant North Sea – Wind farm interaction, The effect of wind farming on mesoscale flow,* ECN, the Neatherlands 2009.
[3] Ivanell S, *Numerical Computations of Wind Turbine Wakes*. PhD thesis, ISBN 978-91-7415-216, KTH Engineering Sciences, Sweden 2009.
[4] Hansen K S, *Guideline to wind farm wake analysis, Guideline to wind farm wake analysis,* Department of Mechanical Engineering, DTU, Denmark 2011.
[5] Sørensen N, *General Purpose Flow Solver Applied to Flow over Hills.* Risø-R-827-(EN), Risø national Laboratory, Denmark 1995.
[6] Michelsen J A, *Basis3D - a platform for development of multiblock PDE solvers. Report AFM 92-05*, Dept. of Fluid Mechanics, DTU, 1992.
[7] Michelsen J A, *Block structured multigrid solution of 2D and 3D elliptic PDE's. Report AFM 94-06*, Dept. of Fluid Mechanics, DTU, 1994.
[8] Ta Phouc L, *Modéles de sous maille appliqués aux écoulmements instationnaires décollés* Tech. rep. LIMSI 93074, LIMSI, France, 1994.
[9] Mikkelsen R, *Actuator Disc Methods Applied to Wind Turbines. MEK-FM-PHD 2003-02,* DTU, Denmark 2003.
[10] Mann J, *Wind field simulation*,Risø, Denmark 1998.
[11] Mikkelsen R, *Prescribed wind shear modelling with the actuator line technique, DTU, Denmark 2007.*
[12] Hansen K S, *WP8:Flow, Deliverable D8.1 Data, Wake measurements used in the model evaluation* DTU ,Denmark 2008.
[13] Matthew J C, *A Method for Designing Generic Wind Turbine Models Representative of Real Turbines And Generic Siemens SWT-2.3-93 and Vestas V80 Specifications* , NREL, the United states of America 2012.